Visual Neuroscience (2000), **17**, 421–436. Printed in the USA.

Response profiles to texture border patterns in area V1

HANS-CHRISTOPH NOTHDURFT,[1,2] JACK L. GALLANT,[1,*] AND DAVID C. VAN ESSEN[1,†]

[1]Division of Biology, California Institute of Technology, Pasadena
[2]Max Planck Institute for Biophysical Chemistry, Department of Neurobiology, Goettingen, Germany

(RECEIVED May 27, 1998; ACCEPTED December 30, 1999)

Abstract

Cells in area V1 of the anesthetized macaque monkey were stimulated with large texture patterns composed of homogeneous regions of line elements (texels) with different orientations. To human observers, such patterns appear to segregate, with the percept of sharp boundaries between texture regions. Our objective was to investigate whether the boundaries are reflected in the responses of single cells in V1. We measured responses to individual texels at different distances from the texture border. For each cell, patterns of optimally or orthogonally orientated texels were adjusted so that only one texel fell into the receptive field and all other texels fell in the visually unresponsive regions outside. In 37 out of 156 neurons tested (24%), texels immediately adjacent to a texture border evoked reliably larger responses than identical texels farther away from the border. In 17 neurons (11%), responses to texels near the border were relatively reduced. Border enhancement effects were generally stronger than border attenuation effects. When tested with four different border configurations (two global orientations and two edge polarities), many cells showed reliable effects for only one or two configurations, consistent with cells encoding information about the orientation of the texture border or its location with respect to the segmented region. Across the sample, enhancement effects were similar for all texture borders. Modulation by the texture surround was predominantly suppressive; even the responses near texture borders were smaller than those to a single line. We compared these results with the results of a popout test in which the line in the receptive field was surrounded by homogeneous texture fields either orthogonal or parallel to the center line. The patterns of response modulation and the temporal onset of differential responses were similar in the two tests, suggesting that the two perceptual phenomena are mediated by similar neural mechanisms.

Keywords: Macaque monkey, Striate cortex, Classical receptive field, Contextual modulation, Texture segmentation, Orientation contrast, Popout

Introduction

This study investigated the neural mechanisms underlying visual segmentation. In textures composed of small line elements (*texels*), regions with texels at different orientations appear to segregate and produce the percept of large homogeneous regions with clear texture boundaries (Beck, 1966, 1982; Olson & Attneave, 1970; Julesz, 1975, 1984; Nothdurft, 1985*b*; Nothdurft & Li, 1985). The same effects are observed when regions are defined by relative motion (Nakayama & Tyler, 1981; Golomb et al., 1985; Nakayama et al., 1985; Nothdurft, 1993) or binocular disparity (Julesz, 1971). These perceptual phenomena are intriguing because these stimuli often do not contain luminance edges, so segmentation must be based on the analysis and comparison of specific texture properties in different parts of the pattern. Visual segmentation and the perception of texture boundaries appear to be closely related to the salience of a single item in a field of dissimilar objects (Nothdurft, 1991, 1992), a phenomenon known as *popout* (Treisman & Gelade, 1980; Treisman, 1985), although some differences between these phenomena have been described (Wolfe, 1992).

The neural basis of texture segmentation remains unclear, but the filter properties of neurons at early cortical processing stages probably play an important role. Many neurons in area V1 are selective for orientation, direction of motion, and binocular disparity (cf. Van Essen, 1985), whereas neurons at earlier processing stages lack these characteristics. Therefore, texels in different regions of a complex texture pattern, differing along these dimensions, should produce differential activation of striate cortical neurons. Borders might then be represented by differences in activity across these cells.

The selective activation of cortical cells by texture properties like texel orientation is well documented (see, for example, Nothdurft & Li, 1985), but it is unclear where the comparison of neuronal activity and the extraction of texture borders might occur. One possibility is that area V1 neurons are modulated by texture information outside the receptive field (RF) and thus encode both

Address correspondence and reprint requests to: Hans-Christoph Nothdurft, Max Planck Institute for Biophysical Chemistry, 37070 Goettingen, Germany. E-mail: hnothdu@gwdg.de

*Present address: Department of Psychology and Program in Neuroscience, 3210 Tolman Hall #1650, U.C. Berkeley, Berkeley, CA 94720-1650, USA.

†Present address: Department of Anatomy and Neurobiology, Washington University School of Medicine, St. Louis, MO 63110, USA.

the feature in the RF (texel orientation) and feature contrast (orientation differences) relative to texels outside the RF (Nothdurft, 1994*a*,*b*). Modulatory effects of this sort have frequently been observed with homogeneous texture surrounds (Allman et al., 1990; Knierim & Van Essen, 1992; DeAngelis et al., 1994; Li & Li, 1994; Sillito et al., 1995; Kastner et al., 1997, 1999; Nothdurft et al., 1999). Many cells in area V1 respond better to texels that contrast with the background than to texels in a uniform texture field (Knierim & Van Essen, 1992; Kastner et al., 1997, 1999; Nothdurft et al., 1999). However, it is unclear whether such modulatory effects also occur with texture boundaries. Lamme (1995) showed that V1 responses in the alert monkey depended on whether the stimulus in the RF was part of a distinct figure or part of a large uniform texture field, but he did not find any effect of the distance of the border. In a related study, Zipser et al. (1996) found that the response differences between figures and homogeneous texture fields generally diminished as the size of the figure increased. But the study did not determine whether response differences were due to the size of the texture region or the distance of texture boundaries from the RF. Lee et al. (1998) recently reported border effects that appeared most pronounced when the borders of the texture figure were parallel to the cell's preferred orientation.

We have measured response modulation in area V1 of anesthetized animals by texture borders at varying distances from the RF. Texture borders were denoted by differential orientation of texels in distinct subregions of a large texture pattern, and patterns were designed and presented in such a way that only one texel fell into the cell's RF. (Preliminary descriptions of these results appeared in Nothdurft et al., 1992; Van Essen et al., 1993, and Gallant et al., 1995.) We compare these findings with data from a popout test in which single lines were surrounded by lines with similar or orthogonal orientation (Nothdurft et al., 1999). The modulatory effects of the surround in the two studies were closely related. The results of the popout study were also consistent with previous studies of the *alert* monkey (Knierim & Van Essen, 1992), suggesting that response modulation by texture boundaries also occurs in alert animals.

Methods

Recordings were made in four anesthetized, paralyzed animals (*Macaca nemestrina*) using standard electrophysiological methods (for details, see Gallant et al., 1996; Nothdurft et al., 1999). All procedures were carried out under institutionally approved protocols and conformed to the NIH Guidelines for the Care and Use of Animals. After an aseptic surgery (implantation of a recording chamber, craniotomy) under general anesthesia (2.5–4.5% isoflurane), anesthesia was maintained throughout the experiment by the continuous intravenous infusion of sufentanil citrate (5–8 μg/kg body weight/h). Appropriate dosage was determined for each animal before the experiment and was adjusted as needed to maintain anesthesia, based on EKG and EEG criteria. After appropriate anesthesia was achieved, animals were paralyzed (gallamine triethiodide; 10 mg/kg/h i.v.) and externally respired through a tracheal cannula. Extracellular single-cell recordings were made with tungsten microelectrodes (Levick style) advanced into the parafoveal representation of area V1. All single units that could be isolated were investigated, and all that gave consistent responses in preliminary testing were studied with the texture border paradigm.

Receptive fields were plotted on a computer monitor using bars whose parameters (size, color, orientation, and position) were optimized for each cell. When the optimal bar stimulus was found, the spatial profile of the RF and the position at which the bar evoked the maximal response were determined along both axes of the bar (see Nothdurft et al., 1999). In all subsequent tests the bar was placed at this optimal position within the RF, at either the optimal or orthogonal orientation.

Texture stimuli

The test patterns contained texels in the optimal and orthogonal orientations (see sketches in Figs. 1–3) and were individually adjusted for each cell. To minimize alignment effects between neighboring lines, texels were arranged in rectangular grids with axes oblique ($\pm 45^\circ$) to texel orientation and hence oblique to the main axes of the RF. The spacing of texels in the grid was adjusted so that only one texel fell into the classical RF and all others appeared in the visually unresponsive regions around the RF. Control tests ensured that the texel spacing was adequate by comparing responses obtained with the RF texel alone and with texture arrays in which the RF texel was removed. The most common texel spacing was 1.5 times the texel length, but smaller (1.2) and larger (2.0) values were used occasionally. To minimize local luminance cues arising from texel orientation differences along the texture borders, the positions of individual texels were varied randomly by up to 20% of the spacing of the texture grid. Texture patterns of this sort have previously been used in psychophysical experiments (Nothdurft, 1985*a*). The jitter was refreshed for each new stimulus presentation, but the texel in the RF always appeared at the previously assessed center position in the RF.

Texture border test

Texels in the optimal or orthogonal orientation were arranged to form large homogeneous texture regions with emergent boundaries between different regions. The texture border test examined the responses of each cell at several different locations relative to these borders (indicated by the circles in Figs. 1–3). Responses were generally assessed for four border configurations oblique to the texel orientation, each presented at varying distances from the RF. We explored two types of texture patterns. *Texture edges* (Fig. 3) were tested in 144 cells; these data form the main body of our analysis of texture boundaries. In a smaller sample of cells we also investigated *texture bars*. Narrow bars (5–7 texels; e.g. Fig. 2) were tested in 16 cells; wide bars (9 texels or more; e.g. Fig. 1) were tested in six cells. Responses obtained when a texture border was adjacent to the cell's RF (the "near border" condition) were compared with those obtained when the border was three (143 cells) or five (13 cells) texels away (the "far border" condition). For 106 cells, we also tested responses at intermediate texel positions (2–4 texels away from the border).

Popout test

For 146 cells, the texture border responses were compared with those obtained in an earlier study of popout effects (Nothdurft et al., 1999). Test patterns resembled a single line in the RF, surrounded by homogeneous texture fields of either orthogonal texels (the "popout" condition) or texels parallel to the single line (the "uniform texture" condition). In a control condition, responses to the single line in the RF were measured with no texture surround. The popout and the texture border tests were typically run in direct sequence for each cell.

Presentation and data acquisition

Stimuli were generated by computer and presented on a 19-inch RGB monitor with 66-Hz frame rate (noninterlaced). Viewing dis-

tance was 114 cm, giving an effective screen size of 18.5 by 14.8 deg of the visual field (1280 by 1024 pixels). Texture patterns covered the whole screen and were shown in one of eight colors (white, dark blue, green, light blue, red, magenta, yellow, and black) selected to produce a good response to a single line over the RF. For each cell, all tests used the same texel color on a neutral background. Luminance variations arising from different line orientations were small and did not produce detectable differences in mean luminance. However, the different colors were not equated for luminance so that the effective texel luminance contrast differed between cells.

Data acquisition was accomplished by a second computer that was synchronized to the stimulus presentation by a photodiode. Data analysis was done off-line. Stimulus presentation time was 0.5 s. Cell activity was recorded from 0.5 s before each stimulus presentation (to measure the spontaneous firing rate of the cell) until 0.5–1 s after stimulus offset, depending on the strength and duration of off responses. Tests contained 12–40 different stimulus conditions shown in pseudorandom order (i.e. all conditions of a particular test were shown once before repetition). There was an interval of at least 3 s between trials.

Data analysis

Most of the analyses presented in this paper are based on the mean responses of each cell over the full period of stimulus presentation, usually averaged over 10–20 repetitions. Responses in the various test conditions were considered to be reliably different when they differed by at least two standard errors of the mean (two-SEM criterion). Using this criterion, fewer than 5% of the cells should show effects by random chance. One analysis classified cells according to their modulation by different border configurations. To compensate for the increased probability of random effects, a three-SEM criterion was used in this part of the analysis. This ensured that the occurrence of chance effects remained below 5%.

Spontaneous firing rates were usually subtracted before analysis. However, for the computation of border enhancement indices (see below), absolute activity levels were used to avoid analytic difficulties (division by zero; high computational noise) arising from the pronounced suppression often observed with homogeneous texture fields (Nothdurft et al., 1999).

Results

We examined texture border responses in 156 cells in area V1. Twenty-four percent of these cells (37/156) responded more strongly when the texture border was adjacent to the RF than when it was three or five steps away. Eleven percent (17/156) showed the opposite pattern, responding more strongly when the texture border was farther away. The remaining cells showed no reliable response variation with respect to border distance.

Examples of response modulation by texture edges

The responses of a cell that was strongly enhanced by the presence of nearby texture borders are shown in Fig. 1. The stimulus was a texture field with a large bar (9 texels wide) at one texel orientation, surrounded by texels at the orthogonal orientation. The stimulus pattern was shown at 19 different positions relative to the RF (as indicated by the circles in the figure). The cell was orientation selective and gave the largest responses when the texels in the RF had the optimal orientation (at positions within the texture bar).

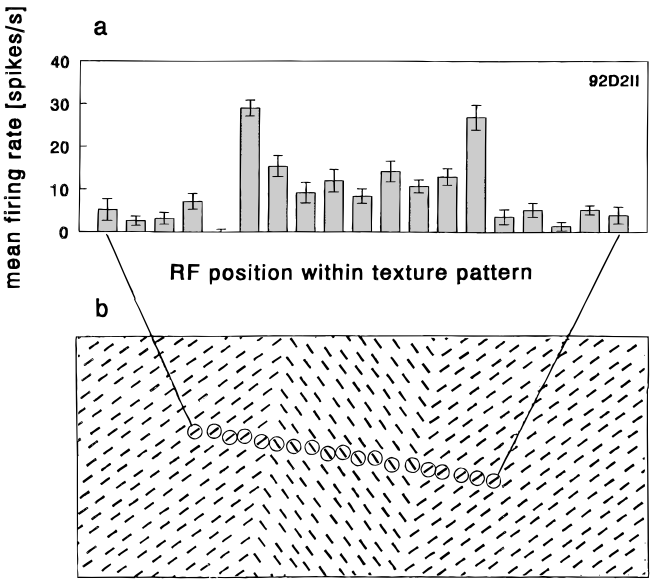

Fig. 1. Responses to texels placed within the RF are modulated by nearby texture borders. (a, b) Stationary texture patterns (b) were presented at various positions on the screen so that the texture borders occurred at different distances from the receptive field (circles). Responses to identical optimally oriented texels within the global texture bar were modulated by the texture surround and increased strongly near texture boundaries. (Preferred orientation: $-35°$; texels were 0.5×0.05 deg, red on dark background.)

However, responses were much stronger when the texture boundary was close to the RF than when it was far away. This led to a relative *enhancement* of responses to texels near the texture border.

Figs. 2 and 3 illustrate the types of responses we encountered and give an overview of the test patterns used. The tests in Fig. 2 were made with bars 5 texels wide at one (Fig. 2a and 2b) or two (Fig. 2d) orientations, thus providing independent measures of border effects for up to four different border configurations. Fig. 2a illustrates a case in which the responses to texels in the middle of the texture bar were only slightly smaller than those to texels near the edges. Texels within the bar and texels outside (at the orthogonal orientation) evoked quite different responses. In this example, cell responses primarily encoded texel orientation with little modulation from texture boundaries. A contrary case is illustrated in Fig. 2b. The responses to texels in the middle of the texture bar were strongly suppressed and were similar to those evoked by the orthogonal texels outside the bar. Texels near the border elicited a larger response. Thus, in this example, cell responses appeared to encode the presence of the texture border to a greater degree than the orientation of individual texels. Many cells showed a mixture of such effects, encoding both texel orientation and nearby texture borders. This is illustrated in Fig. 2d, where the optimally oriented texels within the texture bars evoked stronger responses than the orthogonal texels outside and these responses were further modulated by nearby texture borders. Note that the texels outside the bar also produced border enhancement effects in this cell. The responses to orthogonal texels were generally suppressed, but in two configurations this suppression was reliably smaller near the border.

The cells in Figs. 1 and 2 depict relatively rare cases in which border enhancement occurred with all texture borders tested. Many

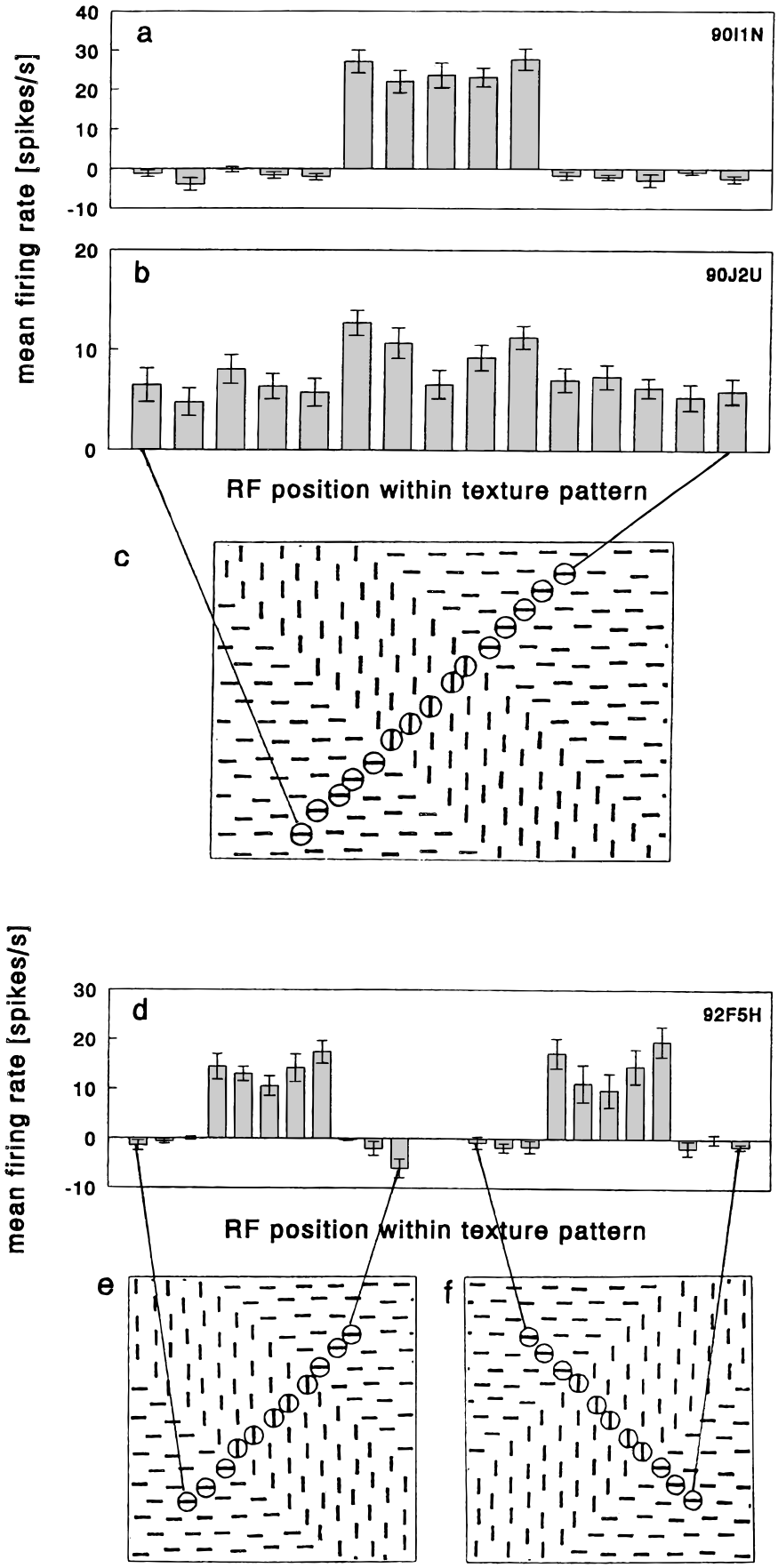

Fig. 2. Responses to texture bars. (a–e) Texture patterns with a global bar at one (c) or two orientations (e) were presented so that individual texels were always centered in the cell's RF (indicated by circles). Mean responses of three different cells (a, b, d) illustrate different degrees of response modulation by texture boundaries. The sketches of stimulus patterns in (c) and (e) are drawn as if cells preferred vertical stimuli. In the actual experiment the size, color, and orientation of texels inside the global bars were optimized for each cell, and the texels outside the bar were always orthogonal copies of these. (Preferred orientations, measured clockwise from vertical, texel sizes and colors for each cell: (a) 140°, 0.55 × 0.1 deg, white; (b) 270°, 0.4 × 0.05 deg, red; and (d) 20°, 1.4 × 0.2 deg, white.)

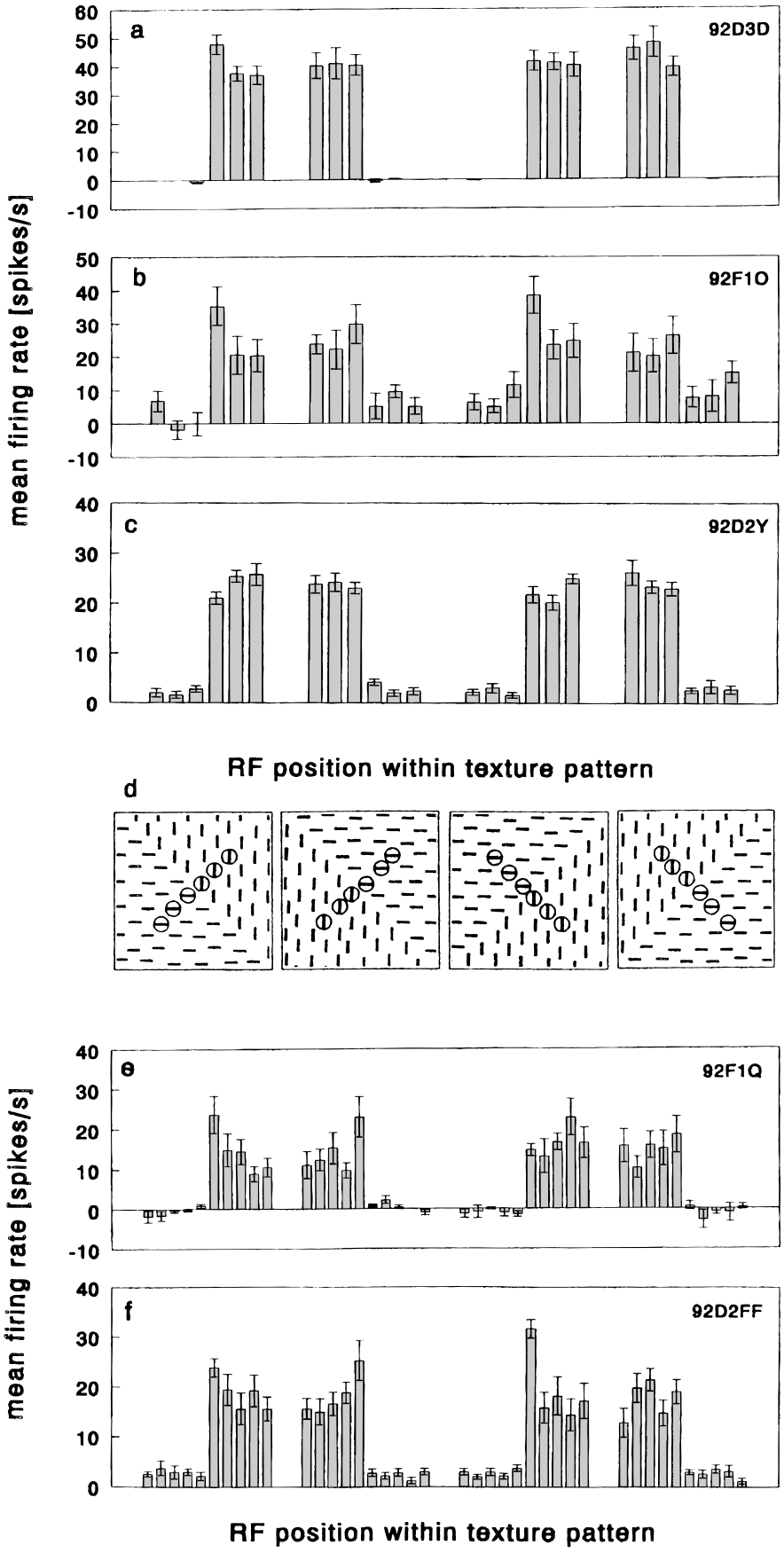

Fig. 3. Responses to texture edges. (a–f) Texture patterns with boundaries in four configurations (d) were presented so that the border appeared at different distances from the cell's RF (circles in d). Responses of selected neurons (a–c, e, f) illustrate the variety of border modulation effects seen in different cells. Responses were obtained at three (a–c) or five (e, f) line positions on either side of the edge. For clarity, the stimulus patterns in (d) are drawn as for a cell with vertical orientation preference. (Preferred orientations, texels sizes, and colors for each cell: (a) 135°, 0.55 × 0.1 deg, red; (b) 90°, 0.4 × 0.1 deg, red; (c) −30°, 1.25 × 0.15 deg, white; (e) 140°, 0.6 × 0.1 deg, red; and (f) −15°, 0.55 × 0.1 deg, red.)

cells showed reliable modulation with only one or two border configurations. The cells in Fig. 3 were tested with texture edges at two orientations and two polarities (analogous to the two edges of a texture bar), and at three (Figs. 3a–3d) or five (Figs. 3e and 3f) texel positions on either side of the edge. Border enhancement was reliable for one (Fig. 3a), two (Figs. 3b and 3e), or three border configurations (Fig. 3f). Failure to show a reliable effect at all tested configurations might reflect signal-to-noise variations among cells having intrinsically symmetric response profiles. Alternatively, this outcome might reflect a biologically significant asymmetry in responses to borders appearing at different locations relative to the RF.

The cell in Fig. 3c showed an effect of the opposite sign: texels near the borders evoked smaller responses than texels farther away. Texture border *attenuation* effects such as this were less frequent and typically less pronounced than enhancement effects.

Response categories

Fig. 4 plots the texture border effects for the entire sample of cells evaluated in our experiments. Most cells were tested with texture edges ($n = 144$), but data are included from 12 cells that were tested only with texture bars. Every cell was tested with four different border configurations (as sketched in Figs. 2d and 3d); each of these individual tests is represented in Fig. 4. For every cell and every tested border configuration, responses to texels near the border are plotted against the responses to the same texels farther away from the border. This analysis was made separately for optimal (Fig. 4a) and orthogonal texel orientations (Fig. 4b). (The data points in Fig. 4 are labeled according to response categories introduced below.) The scatter plots reveal systematic shifts to the lower right quadrant (paired t test; optimal orientation, $t > 4.37$, $P < 0.0001$; orthogonal, $t > 3.11$, $P < 0.002$), indicating that the responses to texels near the border were generally larger than the responses to texels farther away (mean responses: 16.5 ± 0.7 spikes/s *vs.* 15.5 ± 0.6 spikes/s, for the optimal orientations; 5.3 ± 0.4 spikes/s *vs.* 4.6 ± 0.4 spikes/s, for the orthogonal orientations).

To summarize these data and to analyze the scatter in Fig. 4, cells were classified by the number of borders that evoked responses reliably different from those obtained in the far border condition. Fig. 5 shows the distribution of cells in these response categories. Across the entire sample, border enhancement effects were generally more prevalent than border attenuation effects. Reliable enhancement effects with more than one border configuration were seen in 19 cells (12%), for the optimal texel orientation. Reliable attenuation effects with more than one border configuration were seen in only ten cells (6%); none of these produced attenuation effects for more than two border configurations.

The main analysis in Fig. 5 was based on the two-SEM criterion used in related studies (e.g. Knierim & Van Essen, 1992; Nothdurft et al., 1999); only response differences > two SEM were considered as reliable. This criterion ensures that the probability of obtaining border effects by chance (due to random response variations) is small ($P < 0.05$ for each single test). However, the analysis of all four border configurations in a cell considerably increased the probability of obtaining at least one border effect by chance ($P_{4;1} > 0.1$). Therefore, to obtain a conservative estimate of border effects in the one-border categories (one border enhanced or one border attenuated), we also analyzed our data using a more stringent three-SEM criterion. The frequency of border effects un-

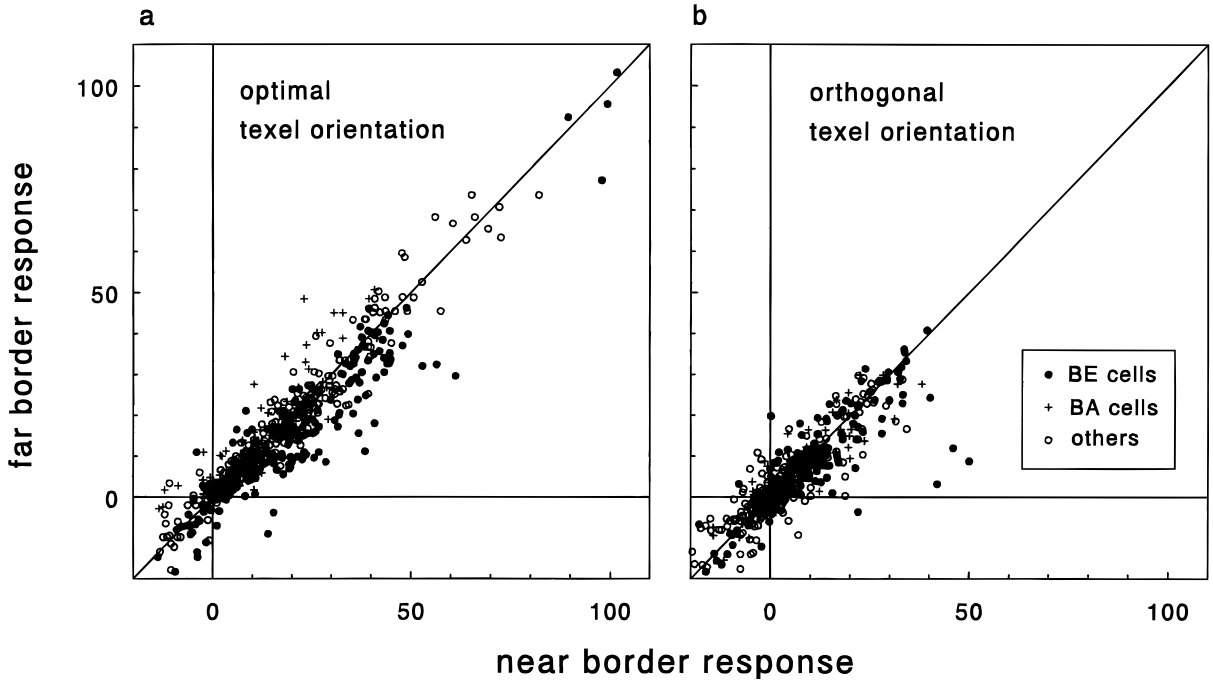

Fig. 4. Responses to texels near *versus* far from the border, for all border configurations tested (four data points per cell). (a) Responses when the texel in the RF had optimal orientation; and (b) responses for orthogonal texels. Near border responses were, on average, larger than far border responses. Cells were classified as showing enhancement (●) or attenuation effects (+) if such effects were reliable for at least one border configuration, or as showing no border effects (○); see text.

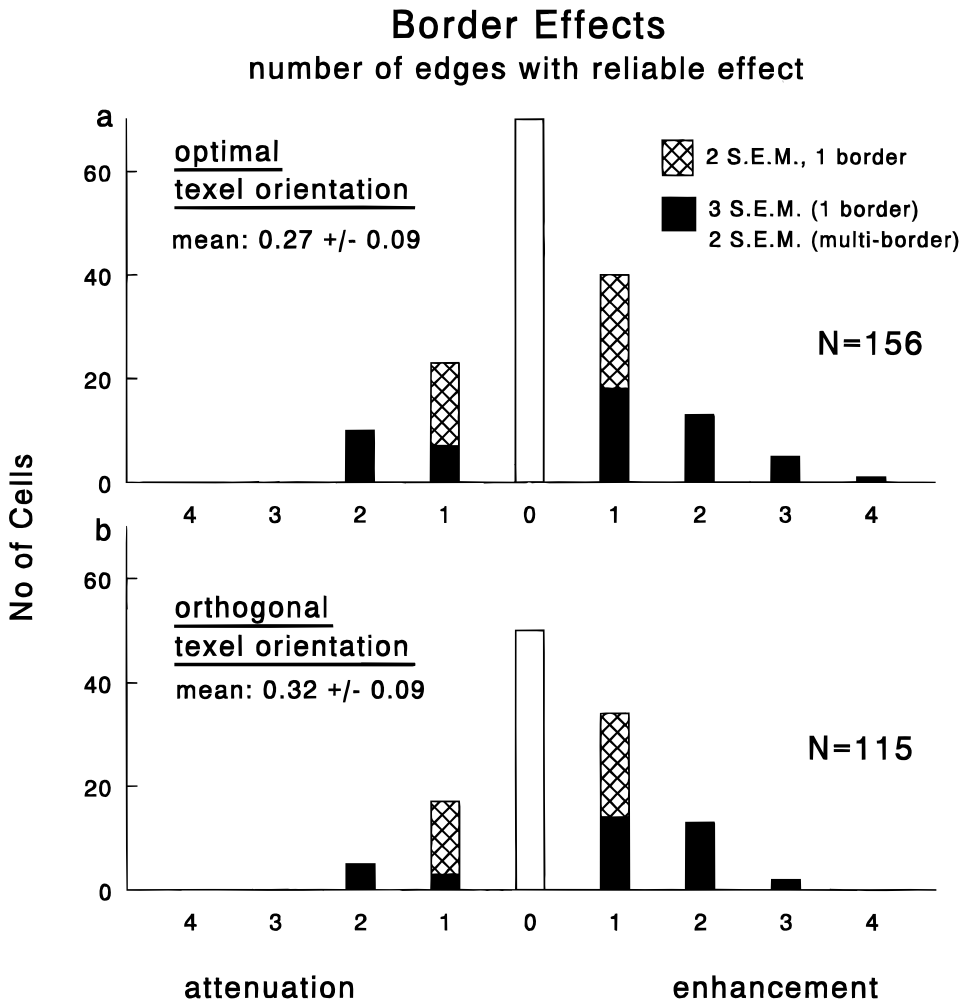

Fig. 5. Distributions of response categories for (a) optimally oriented and (b) orthogonal texels in the RF. Both distributions are biased toward border enhancement effects. Seven cells in panel (a) and six cells in panel (b) were counted twice because different border configurations produced both enhancement and attenuation effects in these cells. Outlines of the histogram represent the analysis based on the two-SEM criterion (see text). A more conservative three-SEM criterion was used for the one-border categories (solid bars); one (a) and two cells (b) were counted twice. Means were computed using a mixture of both criteria, the three-SEM criterion for one-border categories and the two-SEM criterion for multiple-border categories; enhancement effects positive.

der this criterion (solid bars in Fig. 5) is smaller than was found with the two-SEM criterion (hatched bars) but the false positive rate is controlled. With the three-SEM criterion for the one-border categories and the two-SEM criterion for the two-, three- and four-border categories, reliable border enhancement was obtained in 24% (37/156) of the cells, and reliable border attenuation in 11% (17/156) of the cells. The mean of this distribution is significantly shifted toward enhancement effects (one-sided *t*-test; $t > 2.76$, $P < 0.005$).

The analogous distribution for the orthogonal texel orientation is shown in Fig. 5b. (Forty-one cells that responded poorly or not at all to the orthogonal orientation were excluded from analysis.) Responses were generally weaker with orthogonal than with optimally oriented texels in the RF (cf. Fig. 4) but the border effects were similar. Reliable border enhancement was seen in 25% (29/115) of the cells; reliable attenuation effects were seen in only 7% (8/115). In single cells, there was generally little or no correlation between the border effects seen with optimal and orthogonal texel orientations. Border enhancement with optimal texels could be accompanied by border attenuation with orthogonal texels (cf. Fig. 3b) or *vice versa*. However, across the entire sample of cells borders produced the same effects for both texel orientations (paired *t*-test gives $t > 3.31$, $P < 0.001$, for the orthogonal orientation).

Edges vs. bars

Our experiments employed two types of texture fields, edges and bars. The analyses in Figs. 4 and 5 were based mainly on texture edges; only a few cells were tested exclusively with texture bars. However, a recent report suggested that texture responses can depend on the shape or size of the texture field and that figural and non-figure edges might produce different effects (Lee et al., 1998). We therefore compared the responses to texture edges and texture bars in 15 cells. Border enhancement effects (using the two-SEM criterion) were observed in 13 cells with edges and in 12 cells with bars. Border attenuation effects were found in four cells with edges and in four cells with bars; two of these cells showed attenuation with both edges and bars. No cell showed enhancement to one class of stimuli and attenuation to the other class.

Average border responses across the sample

Fig. 6a shows the mean responses of 106 cells that were tested with borders at various distances from the RF; the responses to the three nearest texel positions on either side of the texture edge are shown. For most border configurations, responses to optimally oriented texels adjacent to the border were significantly larger than those to the same texels farther away from the border (paired *t*-tests,

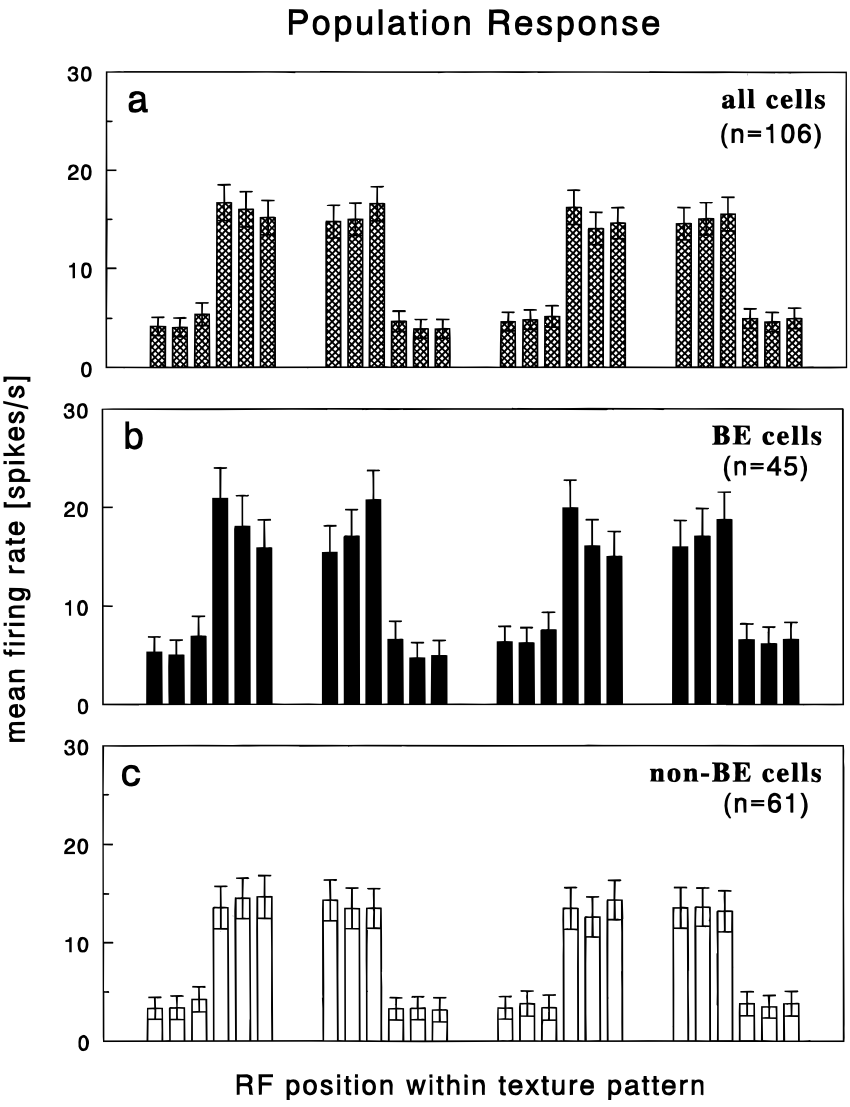

Fig. 6. Mean responses of the cell sample to texture edges. Responses across the four border configurations as in Fig. 3 were averaged over different cell samples: (a) all cells; (b) cells that showed reliable enhancement to at least one of the four border configurations; and (c) all other cells, including cells with border attenuation effects. In the mean responses averaged over cell samples, different border configurations generated similar effects. Vertical bars give the standard error of the mean (SEM). Response differences between near border and far border texels at optimal orientation varied between 1.0 and 1.8 spikes/s in (a), between 2.8 and 5.4 spikes/s in (b), and between 0.3 and 1.1 spikes/s in (c).

$t > 2.42$, $P < 0.02$, except for the rightmost configuration in Fig. 6a, for which differences were not significant). When responses were averaged over all four configurations, the differences between near border and far border texel positions were highly significant ($t > 3.39$, $P < 0.001$). Response differences between near border and far border texel positions varied from 1.0 to 1.6 spikes/s for different border configurations. A similar pattern was observed with orthogonal texels, but response differences were not significant in this case ($P > 0.05$; note, however, that these response differences were significant in the total test sample including all cells and all border configurations; cf. Fig. 4).

To analyze for systematic response differences between cell groups, we classified cells for their response properties in the texture border tests. Cells that showed border enhancement with at least one border configuration at the two-SEM level were classified as "*BE*" cells; cells with border attenuation for one or more border configurations were classified as "*BA*". By definition, border enhancement effects should be stronger in the sample of BE cells, and attenuation effects should be stronger in the sample of BA cells. However, if each group represented a subsample of cells that happened to show enhancement or attenuation effects only by chance, the two cell groups should be symmetrical in their response properties. In addition, if border enhancement and border attenuation were only chance effects and response categories were met only by random response variations in the cells, the effects seen with BE cells should be accompanied by opposite effects of the same magnitude in the complementary cell sample, the "non-BE" cells.

Figs. 6b and 6c compare the responses of BE cells with those of all other cells in the sample (*non-BE* cells). The subset of BE cells showed significant enhancement to texels near the border for every tested configuration (2.8–5.4 spikes/s response difference; $t > 3.29$, $P < 0.005$; optimal orientation). When responses are averaged over different border configurations, response differences are highly significant ($t > 7.24$, $P < 0.0001$). But there was no significant border attenuation in the complementary non-BE cell sample (0.3–1.1 spikes/s; $t < 1.842$, $P > 0.05$), even though cells with clear border attenuation effects were included in this group. Response differences between near border and far border texel position remain nonsignificant when responses to different

border configurations are averaged ($t < 1.92$). Thus, border attenuation effects do not counterbalance the effects of border enhancement in the sample. These data suggest that border enhancement effects are stronger than border attenuation across the population of cells in area V1.

Note that BE cells as a whole show strong enhancement for all border configurations, although in many cells reliable effects were seen for only one or two borders. This suggests that the responses to the different border configurations were not completely independent in individual cells. This is also evident from Fig. 4 in which all four responses of a cell were labeled according to the effects that were found with at least one border configuration. If border effects were highly variable for different configurations in a cell, one might expect a larger scatter of symbols in Fig. 4a than is actually seen. BE cells (filled dots), for example, should be distributed on either side of the line but instead appear to be biased to the lower right side, although there are several exceptions. This order is far less obvious for responses to orthogonal texel orientations (Fig. 4b).

Comparison with single texels and popout

Most cells examined in this study were also evaluated in a separate popout test that was typically performed immediately before or after the texture border test (see Methods). The popout test included the following three conditions: (1) the optimal texel presented alone in the RF, with no texture surround; (2) the optimal texel embedded in a uniform texture field with all texels parallel to that in the RF (the "uniform texture" condition); and (3) the optimal texel surrounded by a homogeneous field of orthogonal texels (the "popout" condition; Nothdurft et al., 1999). Ninety-seven cells of the sample in Fig. 6 were evaluated in this test. Fifteen of these, although responding well to the single texel in the RF, were so strongly suppressed by texture patterns that their mean texture responses fell below the spontaneous firing rates. These cells were excluded from the following analysis. (Excluding these cells from the analyses illustrated in Fig. 6 did not change the overall pattern of results.)

Fig. 7 shows the mean responses of the remaining cells ($n = 82$) averaged over all four border configurations and normalized to the single line response of each cell. All responses to texture were suppressed relative to the single line response. Even texels adjacent to the border, which elicited the largest response, evoked only an average of 67% of the activity obtained with a single line alone (Fig. 7a). (This value was further reduced to 57% when the 15 cells with strong texture suppression were included.) Thus, although responses were enhanced for texels near the border relative to those farther away, they were still suppressed relative to the response to a single texel alone. This result is consistent with earlier reports of the primarily suppressive influence of texture surrounds (Knierim & Van Essen 1992; Nothdurft et al., 1999).

Figs. 7b–7d show the same analysis for different subsamples of cells categorized according to their texture border effects. The sample of BE cells (Fig. 7b) showed strong border enhancement (paired *t*-test; $t = 7.54$, $P < 0.001$) even though individual cells produced reliable enhancement for only one or two border configurations. Non-BE cells (Fig. 7c) did not show any reliable border effect ($P > 0.05$), and in particular none that could compensate for the enhancement of BE cells in the sample. Even in BA cells (cells that showed border attenuation with at least one border configuration; Fig. 7d) the response differences to near and far border texels were not significant ($P > 0.05$) when averaged over all border configurations. Thus, border attenuation was not only less common than border enhancement ($n = 13$ *vs.* $n = 36$) but attenuation effects were also generally smaller than enhancement effects.

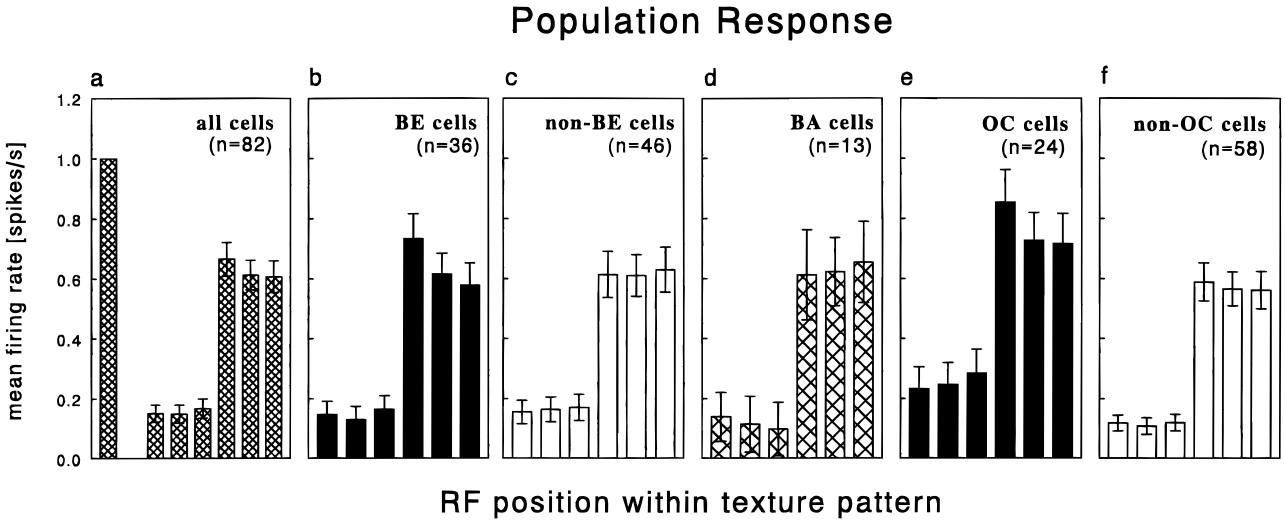

Fig. 7. Mean texture border responses in V1. For each cell, responses for the different border configurations were averaged and normalized with respect to the responses obtained with single lines on a blank field. Histograms show the mean responses of different cell samples at three texel positions on either side of the texture edge. Cells that were completely suppressed by texture fields are not included. All responses to texture were suppressed relative to the single line response. (a) Single line response (left) and means of all cells. (b) Means of BE cells whose responses were enhanced with at least one border configuration. (c) Means of all other (non-BE) cells. (d) Means of BA cells with an attenuation effect for at least one border configuration. (e) Means of cells with preference for orientation contrast in the popout test. (f) Means of all other (non-OC) cells tested for popout effects. Vertical bars give the SEM.

In the popout test, we placed cells into four separate classes according to their response properties (Nothdurft et al., 1999): Orientation contrast (*OC*) cells responded best to the popout condition; uniform texture (*UF*) cells preferred homogeneous texture fields; and generally suppressed (*GS*) cells were suppressed by any texture surround. All other cells were classified as showing no effect (*n.e.*). If border enhancement is caused by the same mechanism that produces orientation contrast effects in the popout test, then it should be particularly pronounced in OC cells. UF cells, on the other hand, should be expected to show primarily border attenuation, and n.e. cells no effect in the border test. As shown in Fig. 7e, OC cells indeed showed pronounced border enhancement in their mean responses (paired *t*-test; $t = 4.59$, $P < 0.001$), whereas the remaining *non-OC* cells did not (Fig. 7f; $t = 1.46$, $P = 0.15$). Table 1 summarizes the relationship between popout and texture border effects in the entire sample of cells. On average, OC cells showed significant border enhancement (mean effects in the right column of Table 1 are significantly different from zero; one-sided *t*-test; $t = 5.0$, $P < 0.001$), while UF cells tended to show border attenuation effects ($t = 1.72$, $P \approx 0.05$). The n.e. cells as a whole were not strongly modulated by texture borders ($t = 1.36$, $P > 0.05$). Thus, responses in the texture border and the popout tests were related in these three cell classes. GS cells, on the other hand, which were strongly suppressed by all texture surrounds in the popout test, showed a more diverse pattern of responses in the border test. Both enhancement and attenuation effects were seen in these cells; enhancement effects predominated ($t = 2.14$, $P < 0.05$). The distribution of GS cells across texture border response categories thus resembles that of the entire cell sample, which was also biased to border enhancement effects ($t = 3.05$, $P < 0.005$).

Quantitative analysis of border effects

We computed several indices to quantify response modulation by texture boundaries. Some of these indices were originally derived for full-field texture surrounds (Knierim & Van Essen 1992; Nothdurft et al., 1999) and were modified for application here.

The Border Enhancement Index, BE, quantifies the enhancement of responses to texels near the border relative to those obtained with texels farther away (three steps, or five if tested). For different border configurations *i*,

$$BE_i = (R'_{\text{near}(i)} - R'_{\text{far}(i)})/R'_{\text{far}(i)}, \quad (1)$$

where R' denotes a neuron's response to a given stimulus condition. (Note that this index is computed with true firing rates as discussed in Methods.) BE values are positive if responses to texels near the border are relatively enhanced and negative if they are relatively attenuated. The values from the four border configurations are averaged to give the mean *BE* index of a cell:

$$BE = \langle BE_i \rangle = (\Sigma BE_i)/4. \quad (2)$$

We computed BE indices on both sides of a texture border, with optimally and nonoptimally oriented texels in the RF. The Generalized Border Enhancement (GBE) index of a cell was defined as the weighted mean of these values:

$$GBE = (BE_{\text{opt}} \cdot R'_{\text{opt}} + BE_{\text{nonopt}} \cdot R'_{\text{nonopt}})/(R'_{\text{opt}} + R'_{\text{nonopt}}). \quad (3)$$

This index quantifies enhancement (positive) and attenuation effects (negative) averaged over all border configurations. If the average near border responses were twice as large as the average far border responses, then the GBE index will equal 1. (For example, the GBE index of the cell in Fig. 3b was 0.25 and that of the cell in Fig. 2d was 1.08.)

The distribution of the GBE indices of all 156 cells in our sample is shown in Fig. 8. The distribution in Fig. 8a is significantly skewed toward border enhancement (one-sided *t*-test; $t = 4.81$; $P < 0.001$). This bias is significant for OC and BE cells (Fig. 8b, 8c; $t = 4.60$, 7.37, respectively, all $P < 0.0005$) and also for non-OC cells in this sample ($t = 3.10$, $P < 0.005$). Non-BE cells did not show a significant bias ($t = 0.05$, $P > 0.05$). Border attenuated (BA) cells produced a negative *GBE* distribution (Fig. 8d;

Table 1. *Distribution of response categories in the border test (columns) and in the popout test (rows) for optimal texel orientation*[a]

	Textures around optimal line elements (156 cells)										
	N borders attenuated					*N* borders enhanced					
	(−)4	(−)3	(−)2	(−)1	0	1	2	3	4	No. of cells	⟨*N*⟩ borders enhanced (⟨*N*⟩ ± SEM)
OC				2	15	9	7	3	1	**35**	0.97±0.19
UF			5	2	8	4				**18**	−0.44±0.26
GS			2	8	23	14	4	2		**52**	0.31±0.14
n.e.			3	9	17	6	1			**34**	−0.21±0.15
?				2	8	7	1			**17**	0.41±0.17
N cells with effect			**10**	**23**	**71**	**40**	**13**	**5**	**1**	**163/156**	**0.27±0.09**

[a]The table includes all 156 cells; seven cells with both enhancement and attenuation effects for different border configurations are listed twice in the left part of the table. The right column gives the mean and the SEM of each distribution (enhancement positive, attenuation negative); different effects in a single cell were averaged for this analysis. OC: cells that preferred orientation contrast; UF: cells that preferred uniform texture; GS: cells whose responses to texture patterns were generally suppressed; n.e.: cells with no reliable popout effect; and ?: cells not tested in the popout paradigm. The response properties observed in the two tests were clearly related: cells that preferred orientation contrast in the popout test also showed the strongest enhancement to texture borders. Cells that preferred uniform textures tended to be attenuated in the presence of a texture border.

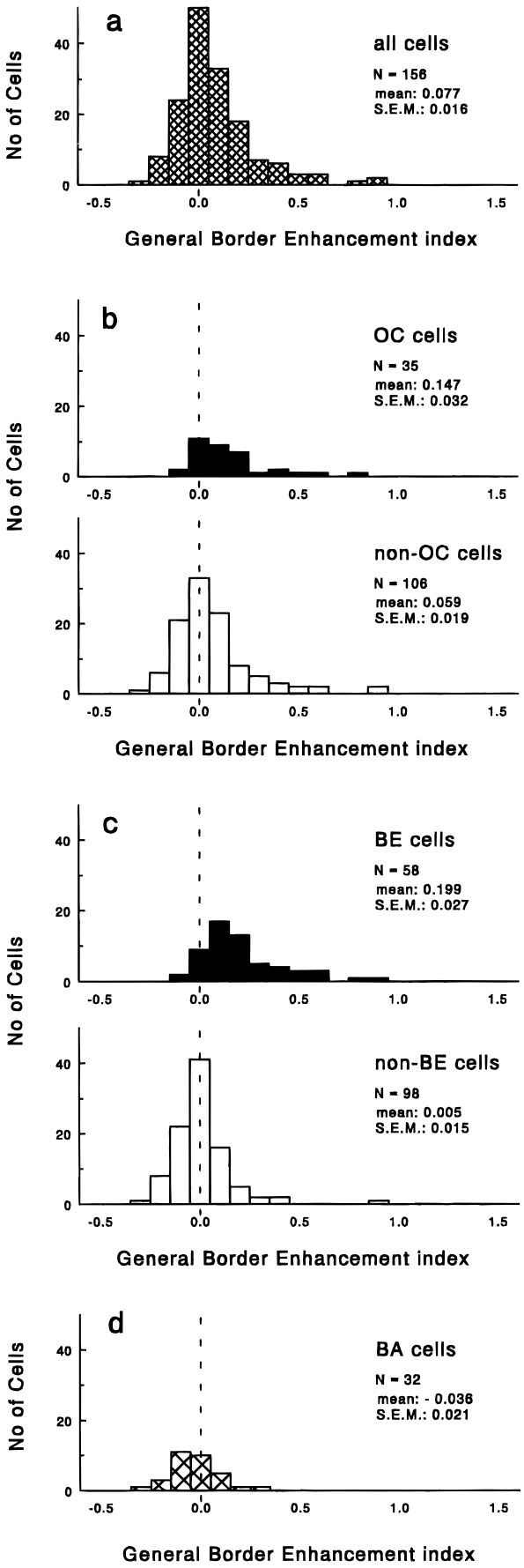

Fig. 8. Distributions of the Generalized Border Enhancement (GBE) indices for different cell groups: (a) the entire sample, (b) OC cells and non-OC cells as identified in the popout test, (c) BE cells (showing border enhancement for at least one border configuration) and non-BE cells, and (d) BA cells (with border attenuation effects for at least one border configuration). The distributions are shifted toward border enhancement (positive values) for all cell groups except non-BE cells (no shift) and BA cells (shift toward border attenuation effects; negative values).

$t = 1.71$, $P < 0.05$). (Note that because the GBE averages over all four border configurations the enhancement obtained with a specific texture border could be much stronger than Fig. 8 suggests.)

Taken together, Figs. 6–8 demonstrate an enhancement of area V1 responses to nearby borders relative to far borders. The effects were most pronounced in BE and OC cells and were not compensated by opposite effects in the complementary cell samples (non-BE cells, non-OC cells). Thus, there is a strong asymmetry in the modulatory effects of texture borders in area V1; enhancement effects are overall larger than attenuation effects.

Comparison with homogeneous surrounds

In the accompanying popout study (Nothdurft et al., 1999), we distinguished two components of texture modulation and quantified them by separate indices (see also Knierim & Van Essen, 1992). The Average Suppression Index (*ASI*) measured the mean suppression from different texture surrounds, while the Differential Firing Index (*DFI*) measured the relative response differences between popout and uniform texture conditions.

$$ASI = 1 - (R_{\text{popout}} + R_{\text{uniform}})/2R_{\text{single line}},$$

$$DFI = (R_{\text{popout}} - R_{\text{uniform}})/R_{\text{single line}}.$$

We have computed similar indices for the border test:

$$ASI^* = 1 - (R_{\text{near}} + R_{\text{far}})/2R_{\text{single line}}, \quad (4)$$

$$DFI^* = (R_{\text{near}} - R_{\text{far}})/R_{\text{single line}}. \quad (5)$$

Although the indices are defined similarly for the two tests, the stimuli themselves were different. In the popout test, all texels in the surround were either similar or orthogonal to the texel in the RF. In contrast, the surround used in the texture border test was always bi-partite. Even in the near border condition, the majority of texels in the surround were identical to the texel in the RF, while fewer than half had the contrasting orientation. Because texels in the surround that are parallel to that in the RF tend to produce the strongest suppression (Knierim & Van Essen, 1992; Nothdurft et al., 1999), we expect suppression effects to be larger, and differential effects smaller in the texture border test than in the popout test. This was indeed the case. Fig. 9 shows the *ASI* and *DFI* values computed for both the border test (abscissa) and the popout test (ordinate) in the same cells. (Only data from stimulus conditions with the optimal texel orientation are shown.) The *ASI* distribution in Fig. 8a is shifted to the lower right, indicating that the ASI^* values obtained from texture border tests were generally larger than the *ASI* values obtained in the popout test (paired *t*-test gives $t = 3.4$, $P < 0.001$ for data points in the central *ASI* ranges;

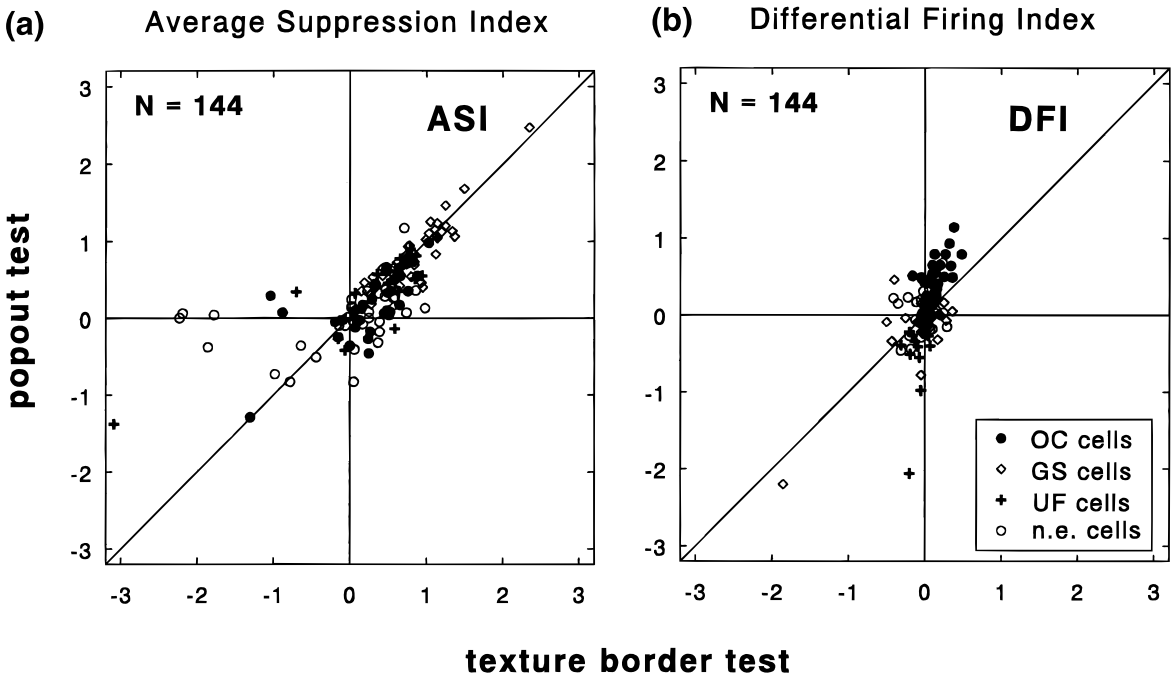

Fig. 9. Texture modulation indices measured with homogeneous texture surrounds (ordinate) or bi-partite textures near the texture border (abscissa). (a) Average Suppression Indices (*ASI*) and (b) Differential Firing indices (*DFI*) as obtained with the optimal texel orientation in the texture border test and in the popout test. The distributions indicate stronger suppression from similar texels than from orthogonal texels in the surround, and a nearly linear relationship between the strength of suppression and the number of similar texels in the nearby surround. Cell labels refer to response categories in the popout test: OC: preference for orientation contrast; GS: generally suppressed; UF: preference for uniform texture; and n.e.: no effect.

$-1.5 \leq ASI \leq 1.5$; $n = 132$). The difference is less pronounced for high *ASI* values because these cells showed strong suppression from both texture surrounds. The correlation between *ASI*s obtained with the two types of stimuli was significant ($r = 0.71$, $P < 0.001$).

Differential effects were about twice as large in the popout test as in the texture border test (Fig. 9b). The slope is slightly greater than 2.0, consistent with the fact that fewer than half of the texels in the texture border surround displayed orientation contrast. Thus, *DFI* values appear to depend directly on the number of orthogonal texels in the surround. Differential effects in both tests were significantly correlated for the sample of OC and UF cells ($r = 0.69$, $P < 0.001$, slope = 2.35), but not for GS cells or n.e. cells. The correlation in the *DFI*s obtained with texture border and popout stimuli suggests that surround effects in these two tests are mediated by common neural mechanisms.

Fig. 10 shows the analogous analysis for texels at intermediate positions, one step away from the border. (Responses to these intermediate positions replace the near border responses in eqns. (4) and (5). Since intermediate positions were not tested in all cells, the sample is smaller than that plotted in Fig. 9.) The *ASI* distributions for popout and texture borders in Fig. 10a differ significantly (paired *t*-test: $t = 3.68$, $P < 0.001$), reflecting the generally stronger suppression from texture surrounds in the texture border test ($r = 0.81$, $P < 0.001$). However, differential effects from the more distant border configuration are almost nonexistent (cf. Fig. 10b). Thus, border effects were only pronounced for texels immediately adjacent to the border (cf. Fig. 7).

Timing analysis

Temporal response characteristics were analyzed in all BE cells that gave brisk responses at stimulus onset. (The analysis shown here is based on the original cell responses, but similar results were obtained when the cell responses were normalized to the mean activity in the near border condition.) Fig. 11a illustrates the near and far border responses, averaged over all four border configurations for the population of BE cells. Stimulus evoked activity began about 40 ms after stimulus onset, and the near and far border responses diverged about 20 ms later. To verify the time course of this difference, we compared the average near and far border responses in all 20-ms time windows encompassing the stimulus period (see Fig. 11b). Near and far border responses were not significantly different in any time windows before 60 ms after stimulus onset (paired *t*-test, $t < 1.21$, $P > 0.05$), but they were significantly different in all later time windows ($t > 3.13$, $P < 0.005$). The observed delay of border enhancement effects is similar to the delay observed with popout and uniform texture patterns (Nothdurft et al., 1999), suggesting that the explicit representation of texture boundaries and popout targets occurs after initial responses to the texture stimulus itself.

Discussion

Our data show that responses in V1 can be strongly modulated by texture borders near the classical RF. In 24% of the cells, responses to texels immediately adjacent to a texture border were

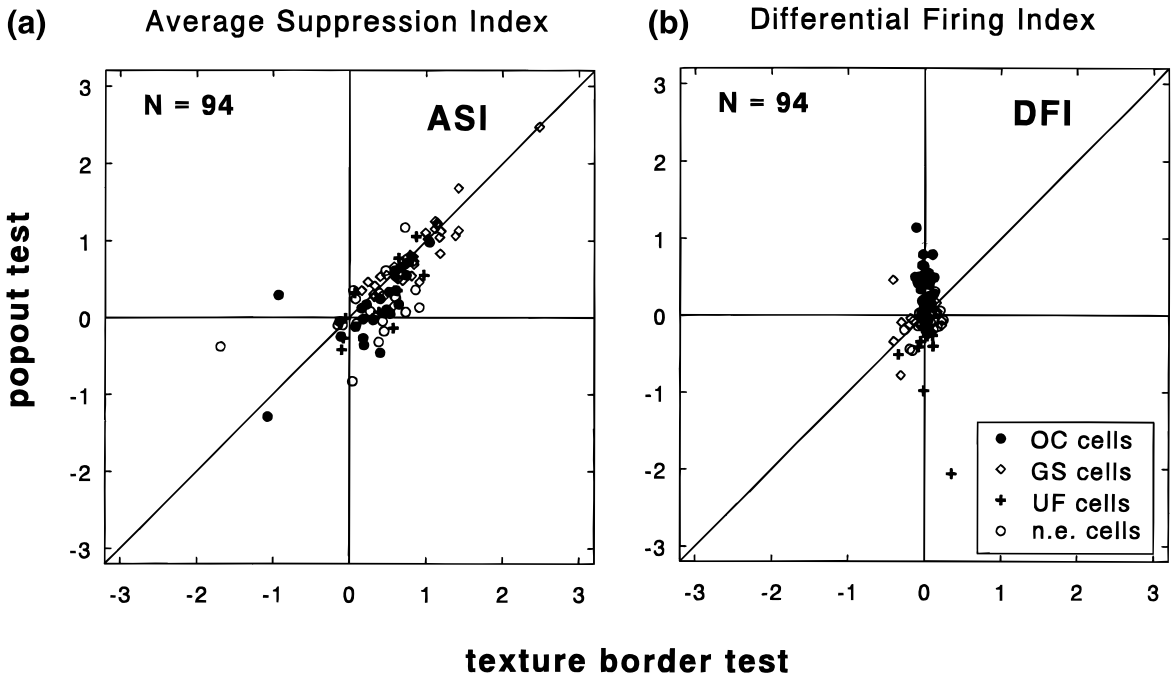

Fig. 10. Texture modulation indices as in Fig. 9 obtained when the texture boundaries were farther from the RF. In these plots, texture border indices were computed for texels in the second row from the border. While the average suppression was still pronounced, differential (border) effects almost vanished at this distance.

larger than the responses to texels farther away. An additional 11% of cells showed response attenuation to borders near the RF, but these effects were generally weaker. The strength of modulation in individual cells often depended on the orientation of the border, perhaps reflecting asymmetries in the RF surround (Walker et al., 1997). However, the average responses of all V1 cells in the sample showed enhancement effects for all border configurations.

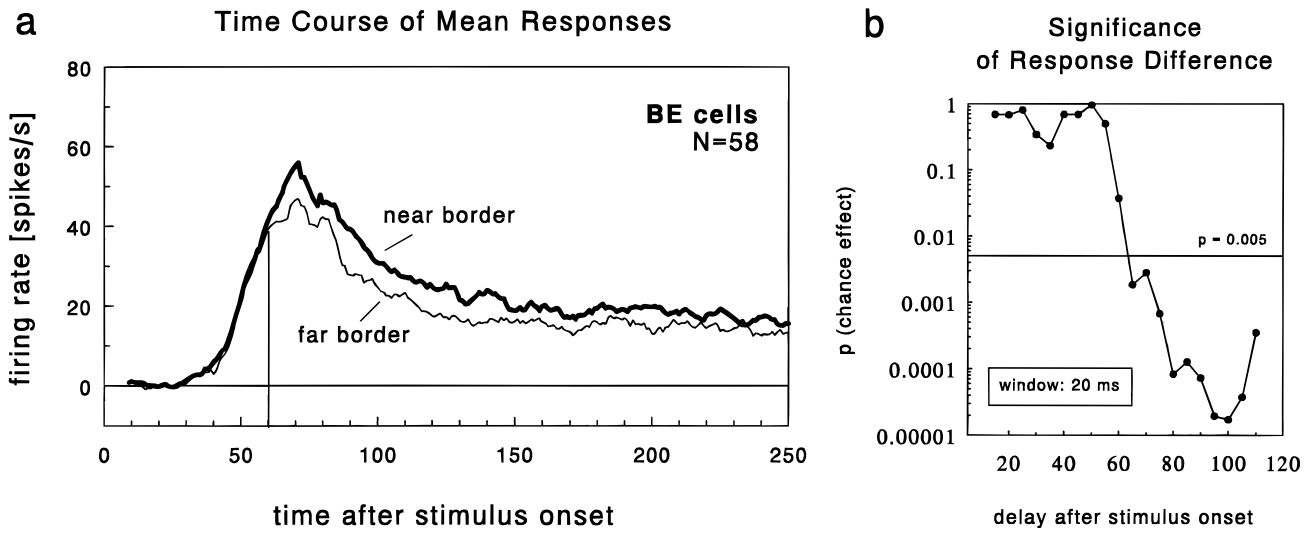

Fig. 11. (a) Time course of the mean responses of BE cells to texels near *versus* far from the border. Responses begin to diverge about 60 ms after stimulus onset and about 15–20 ms after response onset. The histograms shown here had a bin width of 1 ms and were smoothed with a 7-ms rectangular window. (b) Evaluation of significance using paired *t*-test analysis. For different delays after stimulus onset (abscissa), responses in a 20-ms time window were averaged and compared. Response differences were generally not significant for time windows before the 60-ms delay and generally significant for time windows thereafter.

Figure and ground

These findings are particularly noteworthy, as they were obtained in anesthetized animals. Several recent studies of area V1 conducted in alert primates found increased responses to textural figures compared to identical stimuli contained in textural background (Lamme, 1995; Zipser et al., 1996; Lee et al., 1998), but these effects were reported to disappear under anesthesia (Zipser et al., 1997). However, in some of these studies, it remained unclear whether the increased responses to figures were due to response modulation by texture borders or reflected active perceptual figure-ground segmentation. While there is evidence from psychophysics (e.g. Nothdurft, 1985*b*, 1992, 1994*b*, 1997) and eye movement studies (Deubel et al., 1988) that texture boundaries are crucial for the detection of texture figures, some cells in the earlier alert monkey studies showed increased responses regardless of their position within the figure. In contrast, the present data from anesthetized animals demonstrated clear modulation by nearby texture borders, but did not confirm the figural "interior enhancement" effects reported in the studies on alert animals (Lamme, 1995; Zipser et al., 1996; Lee et al., 1998). Only the recent alert monkey study of Lee et al. (1998) distinguished between enhancement effects observed near texture boundaries and those related to the size and form of texture figures. In that study, texture border enhancement effects were most pronounced when the border was parallel to the cell's preferred orientation. To avoid confounds related to texel alignment (Beck et al., 1989; Field et al., 1993; Polat & Sagi, 1993; Kapadia et al., 1995), our texture borders were always oblique to the cell's preferred orientation. Even so, we found that border enhancement effects were clearly visible and were quite strong in some cells.

Lee et al. (1998) also reported increased responses at the center axes of square- or bar-shaped texture figures in some cells. The authors related this observation to analogous perceptual effects observed in humans (Kovacs & Julesz, 1994). We did not observe reliable effects of this sort in anesthetized animals (but have tested only a small sample of cells with bar-shaped stimuli). However, with respect to border effects we did not see any systematic differences between texture bar and texture edge stimuli, suggesting that border effects, unlike center effects, do not depend on the size of the texture figure. This is in agreement with the observations of Lee et al. (1998).

Neuronal representation of texture borders

It is commonly assumed that contours defined by luminance contrast are extracted in area V1 and that their local orientation is explicitly represented in the activity of neurons at this level. Since orientation contrast can be detected only by comparing local orientation across space, one might have predicted that texture borders defined by orientation contrast would be represented in higher visual areas where the orientation-specific responses of V1 cells could be compared. Contrary to this prediction, but in agreement with evoked potential studies (Bach & Meigen, 1992; Lamme et al., 1992, 1993), our data suggest that contours defined by orientation contrast are also represented in V1.

This observation has several important implications for models of visual segmentation. First, response modulation by feature contrast provides a simple mechanism to extract borders from more complex textures (Nothdurft, 1994*a*, 1997). Local orientation contrast will enhance the responses near a texture border, irrespective of the orientation of the constituent texels; thus, borders made of different texel orientations are represented by similar variations in the *mean responses* in V1. Second, if texture borders defined by luminance and orientation contrast are represented at the same level of processing, then both types of contours might be represented similarly at higher stages of processing. This could explain why texture borders defined by multiple dimensions can generate the percept of a single homogeneous boundary (Nothdurft, 1994*b*). Contextual modulation in V1 is produced by many texture dimensions including differences in motion, color, and binocular disparity (Allman et al., 1990; Knierim & Van Essen, 1992; DeAngelis et al., 1994; Li & Li, 1994; Sillito et al., 1995; Zipser et al., 1996; Kastner et al., 1997, 1999). Therefore, this effect may generalize to dimensions other than orientation that also produce the percept of homogeneous regions delimited by sharp texture boundaries (Cavanagh et al., 1990; Nothdurft, 1993, 1994*b*, 1995).

The modulatory effects of texture borders do not necessarily imply that the *orientation* of these borders is represented explicitly in area V1. Although the border effects we observed often varied for different configurations, so V1 cells might represent either border orientation or their position relative to a segmented region; the global border orientation might also be extracted elsewhere. Merigan et al. (1993) found that V2 lesions in the macaque reduced the ability to discriminate the orientation of texture bars (defined by orientation contrast) but did not affect the detection of popout from orientation. Thus, discrimination of texture borders may occur at a later stage of processing than area V1.

Parallels to visual popout

The modulatory effects of texture surrounds have previously been studied using homogeneous texture fields. Neurons in V1 generally respond less strongly to texels surrounded by similar texels than to the same texels when surrounded by texels at the orthogonal orientation (Knierim & Van Essen, 1992; Kastner et al., 1997, 1999; Nothdurft et al., 1999). Because texels in orthogonal surrounds are highly salient and "pop out" (Treisman, 1985; Treisman & Gormican, 1988; Foster & Ward, 1991; Nothdurft, 1991, 1992), it has been proposed (Knierim & Van Essen, 1992; Nothdurft, 1991, 1994*a*; Kastner et al., 1997) that perceptual popout could be based on the surround modulation observed in area V1. Similar surround enhancement effects might account for the detection of texture boundaries (Nothdurft, 1994*b*).

Psychophysical studies have shown that popout and texture segmentation share many properties. For example, both phenomena depend on local orientation contrast (Nothdurft, 1991, 1992). In the present study, we found a clear relationship between modulation by homogeneous texture fields and by texture borders. Border enhancement and popout effects were linearly related in many cells (cf. Fig. 9), and the strength of both effects depended mainly on the number of contrasting texels in the immediate surround of the RF. In addition, differences in the time course of responses obtained with texels nearer and farther from the texture borders (Fig. 11) were similar to those found with popout and uniform texture fields (Nothdurft et al., 1999). These parallels suggests that both perceptual phenomena are mediated by similar neural mechanisms.

The enhanced responses to nearby borders were usually smaller than the responses obtained for a single line, suggesting that border enhancement is not due to specific facilitatory effects (cf. Maffei & Fiorentini, 1976; Sillito et al., 1995). Instead, these effects may be due to orientation-dependent inhibition (e.g. stronger suppression for similar texels in the surround) or disinhibition (e.g. weaker suppression from orthogonal texels in the surround), or perhaps a combination of both. Either of these mechanisms could be implemented *via* long-range connections

within V1 (Rockland & Lund, 1983; Gilbert & Wiesel, 1989) or *via* feedback from higher areas.

Feature linking and alignment

Our data suggest that local feature contrast is sufficient to allow texture segmentation (Nothdurft, 1991, 1994*b*) and that segmentation does not require the active grouping of similar elements by feature linking processes (cf. Singer, 1985; Eckhorn et al., 1988). Local orientation contrast increases the activity of cells near texture borders and hence "marks" the course of texture borders in V1.

However, other perceptual phenomena might be consistent with feature linking mechanisms. For example, the perceived continuation of a long path of locally similar line elements in a texture field (Field et al., 1993; Moulden, 1994) or of aligned squares (Beck et al., 1989) suggests the existence of mechanisms that detect colinearity and alignment (see also Polat & Sagi, 1993). Kapadia et al. (1995) verified that responses of V1 cells are enhanced when a bar in the RF is aligned with another bar of similar orientation in the near surround. Our stimuli were not appropriate for testing such effects because the nearest texels were always placed oblique to the main axis of the RF (cf. Figs.1–3). Thus, our data reflect the general effects of modulation from a texture surround, but do not address specific interactions from local regions of the surround. The modulatory effects we have observed appeared to depend mainly on the number of contrasting texels nearby; systematic variations with texture border orientation were not seen. However, there is psychophysical evidence that such variations do occur (Nothdurft, 1992; Wolfson & Landy, 1995). Interactions between the global orientation of texture borders and the local orientation of texture elements thus remain an important issue for future single cell studies.

Acknowledgments

The work was supported by NATO Collaborative Research Grant CRG 890920 and by ONR Grant N00014089-J-1192.

References

Allman, J., Miezin, F. & McGuinness, E.L. (1990). Effects of background motion on the responses of neurons in the first and second cortical visual areas. In *Signal and Sense: Local and Global Order in Perceptual Maps,* ed. Edelman, G.M., Gall, W.E. & Cowan, M.W., pp. 131–142. New York: Wiley-Liss.

Bach, M. & Meigen, T. (1992). Electrophysiological correlates of texture segregation in the human visual evoked potential. *Vision Research* **32**, 417–424.

Beck, J. (1966). Perceptual grouping produced by changes in orientation and shape. *Science* **154**, 538–540.

Beck, J. (1982). Textural segmentation. In *Organization and Representation in Perception,* ed. Beck, J., pp. 285–317. Hillsdale, New Jersey: Erlbaum.

Beck, J., Rosenfeld, A. & Ivry, R. (1989). Line segregation. *Spatial Vision* **4**, 75–101.

Cavanagh, P., Arguin, M. & Treisman, A. (1990). Effect of surface medium on visual search for orientation and size features. *Journal of Experimental Psychology: Human Perception and Performance* **16**, 479–491.

DeAngelis, G.C., Freeman, R.D. & Ohzawa, I. (1994). Length and width tuning of neurons in the cat's primary visual cortex. *Journal of Neurophysiology* **71**, 347–374.

Deubel, H., Findlay, J. M., Jacobs, A. & Brogan, B. (1988). Saccadic eye movements to targets defined by structure differences. In *Eye Movement Research: Physiological and Psychological Aspects,* ed. Lüer, G., Lass, U. & Shallo-Hoffman, J., pp. 107–145. Göttingen: Hogrefe.

Eckhorn, R., Bauer, R., Jordan, W., Brosch, M., Kruse, W., Munk, M. & Reitboeck, H.J. (1988). Coherent oscillations: A mechanism of feature linking in the visual cortex? *Biological Cybernetics* **60**, 121–130.

Field, D.J., Hayes, A. & Hess, R.F. (1993). Contour integration by the human visual system: Evidence for a local "association field". *Vision Research* **33**, 173–193.

Foster, D.H. & Ward, P.A. (1991). Asymmetries in oriented-line detecion indicate two orthogonal filters in early vision. *Proceedings of the Royal Society B* (London) **243**, 75–81.

Gallant, J.L., Van Essen, D.C. & Nothdurft, H.C. (1995). Two-dimensional and three-dimensional texture processing in visual cortex of the macaque monkey. In *Early Vision and Beyond*, ed. Papathomas, T.V., Chubb, C., Gorea, A. & Kowler, E., pp. 89–98. Cambridge, Massachusetts: MIT Press.

Gallant, J.L., Connor, C.E., Rakshit, S., Lewis, J.W. & Van Essen, D.C. (1996). Neural responses to polar, hyperbolic, and Cartesian gratings in area V4 of the macaque monkey. *Journal of Neurophysiology* **76**, 2718–2739.

Gilbert, C.D. & Wiesel, T.N. (1989). Columnar specificity of intrinsic horizontal and corticocortical connections in cat visual cortex. *Journal of Neuroscience* **9**, 2432–2442.

Golomb, B., Andersen, R.A., Nakayama, K., MacLeod, D.I.A. & Wong, A. (1985). Visual thresholds for shearing motion in monkey and man. *Vision Research* **25**, 813–820.

Julesz, B. (1971). *Foundations of the Cyclopean Perception*. Chicago, Illinois: University Press.

Julesz, B. (1975). Experiments in the visual perception of texture. *Scientific American* **232**(4), 34–43.

Julesz, B. (1984). A brief outline of the texton theory of human vision. *Trends in Neuroscience* **7**, 41–45.

Kapadia, M.K., Ito, M., Gilbert, C.D. & Westheimer, G. (1995). Improvement in visual sensitivity by changes in local context: Parallel studies in human observers and in V1 of alert monkeys. *Neuron* **15**, 843–856.

Kastner, S., Nothdurft, H.C. & Pigarev, I.N. (1997). Neuronal correlates of pop-out in cat striate cortex. *Vision Research* **37**, 371–376.

Kastner, S., Nothdurft, H.C. & Pigarev, I.N. (1999). Neuronal responses to orientation and motion contrast in cat striate cortex. *Visual Neuroscience* **16**, 587–600.

Knierim, J.J. & Van Essen, D.C. (1992). Neuronal responses to static texture patterns in area V1 of the alert macaque monkey. *Journal of Neurophysiology* **67**, 961–980.

Kovacs, I. & Julesz, B. (1994). Perceptual sensitivity maps within globally defined visual shapes. *Nature* **870**, 644–646.

Lamme, V.A.F. (1995). The neurophysiology of figure-ground segregation in primary visual cortex. *Journal of Neuroscience* **15**, 1605–1615.

Lamme, V.A.F., Van Dijk, B.W. & Spekreijse, H. (1992). Texture segregation is processed by primary visual cortex in man and monkey. Evidence from VEP experiments. *Vision Research* **32**, 797–807.

Lamme, V.A.F., Van Dijk, B.W. & Spekreijse, H. (1993). Organization of texture segregation processing in primate visual cortex. *Visual Neuroscience* **10**, 781–790.

Lee, T.S., Mumford, D., Romero, R. & Lamme, V.A.F. (1998). The role of the primary visual cortex in higher level vision. *Vision Research* **38**, 2429–2454.

Li, C.Y. & Li, W. (1994). Extensive integration field beyond the classical receptive field of cat's striate cortical neurons—classification and tuning properties. *Vision Research* **34**, 2337–2355.

Maffei, L. & Fiorentini, A. (1976). The unresponsive regions of visual cortical receptive fields. *Vision Research* **16**, 1131–1139.

Merigan, W.H., Nealey, T.A. & Maunsell, J.H.R. (1993). Visual effects of lesions of cortical area V2 in macaques. *Journal of Neuroscience* **13**, 3180–3191.

Moulden, B. (1994). Collator units: Second-stage orientational filters. In *Higher-Order Processing in the Visual System,* ed. Bock, G.R. & Goode, J.A., pp. 170–192. Chichester: J.A. Wiley (Ciba Foundation Symposium 184).

Nakayama, K. & Tyler, C.W. (1981). Psychophysical isolation of movement sensitivity by removal of familiar position cues. *Vision Research* **21**, 427–433.

Nakayama, K., Silverman, G.H., MacLeod, D.I.A. & Mulligan, J. (1985). Sensitivity to shearing and compressive motion in random dots. *Perception* **14**, 225–238.

Nothdurft, H.C. (1985*a*). Orientation sensitivity and texture segmentation in patterns with different line orientation. *Vision Research* **25**, 551–560.

NOTHDURFT, H.C. (1985*b*). Sensitivity for structure gradient in texture discrimination tasks. *Vision Research* **25**, 1957–1968.
NOTHDURFT, H.C. (1991). Texture segmentation and pop-out from orientation contrast. *Vision Research* **31**, 1073–1078.
NOTHDURFT, H.C. (1992). Feature analysis and the role of similarity in pre-attentive vision. *Perception and Psychophysics* **52**, 355–375.
NOTHDURFT, H.C. (1993). The role of features in preattentive vision: Comparison of orientation, motion, and color cues. *Vision Research* **33**, 1937–1958.
NOTHDURFT, H.C. (1994*a*). Cortical properties of preattentive vision. In *Structural and Functional Organization of the Neocortex*, ed. ALBOWITZ, B., ALBUS, K., KUHNT, U., NOTHDURFT, H.C. & WAHLE, P., pp. 375–384. Heidelberg: Springer.
NOTHDURFT, H.C. (1994*b*). On common properties of visual segmentation. In *Higher-Order Processing in the Visual System*, ed. BOCK, G.R. & GOODE, J.A., pp. 245–268. Chichester: J.A. Wiley (Ciba Foundation Symposium 184).
NOTHDURFT, H.C. (1995). Generalized feature contrast in preattentive vision. *Perception* **24**, 22.
NOTHDURFT, H.C. (1997). Different approaches to the coding of visual segmentation. In *Computational and Biological Mechanisms of Visual Coding*, ed. JENKINS, M. & HARRIS, L., pp. 20–43, New York: Cambridge University Press.
NOTHDURFT, H.C. & LI, C.Y. (1985). Texture discrimination: Representation of orientation and luminance differences in cells of the cat striate cortex. *Vision Research* **25**, 99–113.
NOTHDURFT, H.C., GALLANT, J.L. & VAN ESSEN, D.C. (1992). Neural responses to texture borders in macaque area V1. *Society for Neuroscience Abstract* **18**(2), 1275.
NOTHDURFT, H.C., GALLANT, J.L. & VAN ESSEN, D.C. (1999). Response modulation by texture surround in primate area V1: Correlates of "pop-out" under anesthesia. *Visual Neuroscience* **16**, 15–34.
OLSON, R.K. & ATTNEAVE, F. (1970). What variables produce similarity grouping? *American Journal of Psychology* **83**, 1–21.
POLAT, U. & SAGI, D. (1993). Lateral interactions between spatial channels: Suppression and facilitation revealed by lateral masking experiments. *Vision Research* **33**, 993–999.
ROCKLAND, K.S. & LUND, J.S. (1983). Intrinsic laminar lattice connections in primate visual cortex. *Journal of Comparative Neurology* **216**, 303–318.
SILLITO, A.M., GRIEVE, K.L., JONES, H.E., CUDEIRO, J. & DAVIS, J. (1995). Visual cortical mechanisms detecting focal orientation discontinuities. *Nature* **378**, 492–496.
SINGER, W. (1985). The putative role of synchrony in cortical processing. *Vision Research* **25**, 1297–1304.
TREISMAN, A. (1985). Preattentive processing in vision. *Computer Vision, Graphics, and Image Processing* **31**, 156–177.
TREISMAN, A.M. & GELADE, G. (1980). A feature-integration theory of attention. *Cognitive Psychology* **12**, 97–136.
TREISMAN, A. & GORMICAN, S. (1988). Feature analysis in early vision: Evidence from search asymmetries. *Psychological Review* **95**, 15–48.
VAN ESSEN, D.C. (1985). Functional organization of primate visual cortex. In *Cerebral Cortex*, ed. JONES, E.G. & PETERS, A., pp. 259–329. New York: Plenum.
VAN ESSEN, D.C., GALLANT, J. & NOTHDURFT, H.C. (1993). Texture processing in striate and extrastriate cortex of the Macaque monkey. *Spatial Vision* **7**, 84.
WALKER, G.A., OHZAWA, I. & FREEMAN, R.D. (1997). Asymmetrical suppression in receptive field surrounds of neurons in the cat's striate cortex. *Investigative Ophthalmology and Visual Science* **38**, S968.
WOLFE, J.M. (1992). "Effortless" texture segmentation and "parallel" visual search are not the same thing. *Vision Research* **32**, 757–763.
WOLFSON, S.S. & LANDY, M.S. (1995). Discrimination of orientation-defined texture edges. *Vision Research* **35**, 2863–2877.
ZIPSER, K., LAMME, V.A.F. & SCHILLER, P.H. (1996). Contextual modulation in primary visual cortex. *Journal of Neuroscience* **16**, 7376–7389.
ZIPSER, J., LAMME, V.A.F. & SPEKREIJSE, H. (1997). Figure/ground signals in V1 eliminated by anesthesia. *Investigative Ophthalmology and Visual Science* **38**, S969.